Journal of Power Sources 244 (2013) 222–233

Contents lists available at SciVerse ScienceDirect

Journal of Power Sources

journal homepage: www.elsevier.com/locate/jpowsour

Synthesis of $Li[Ni_{0.2}Li_{0.2}Mn_{0.6}]O_2$ nano-particles and their surface modification using a polydopamine layer

Hye Jin Lee, Yong Joon Park*

Department of Advanced Materials Engineering, Kyonggi University, San 94-6, Yiui-dong, Yeongtong-gu, Suwon, Gyeonggi-do 443-760, Republic of Korea

HIGHLIGHTS

- Polydopamine was successfully used as a binding agent for coating of cathode.
- The high reactivity of the polydopamine layer aided adhesion with the ZrO_2 coating.
- It also helped in its homogeneous dispersion of coating material.
- The ZrO_2 coating suppressed side reactions with the electrolyte.
- And protected the surface of $Li[Ni_{0.2}Li_{0.2}Mn_{0.6}]O_2$-based cathode.

ARTICLE INFO

Article history:
Received 13 November 2012
Received in revised form
21 January 2013
Accepted 28 January 2013
Available online 5 February 2013

Keywords:
Nano-particle
Cathode
Lithium battery
Surface coating
Polydopamine

ABSTRACT

$Li[Ni_{0.2}Li_{0.2}Mn_{0.6}]O_2$ nanoparticles are fabricated using a combustion method in which three different dispersing agents, gelatin, urea and Pluronic® P-123 (P123), are introduced as dispersing agents. The dispersing agents are used in order to disperse the primary particles during the sol–gel thermolysis process and reduce the sizes of the powder particles. Reducing the size of the particles is effective in improving the rate capability of the $Li[Ni_{0.2}Li_{0.2}Mn_{0.6}]O_2$ electrode. However, the cyclic performance deteriorates due to vigorous side reactions with the electrolyte. In order to avoid this, the surfaces of the $Li[Ni_{0.2}Li_{0.2}Mn_{0.6}]O_2$ nanoparticles, prepared using dispersing agents, are modified by a ZrO_2 surface coating. A novel precoating of polydopamine is used to aid the ZrO_2 coating of the nanosized particles. The surfaces of the coated $Li[Ni_{0.2}Li_{0.2}Mn_{0.6}]O_2$ particles are homogeneously covered with the ZrO_2, demonstrating the effectiveness of the polydopamine precoating as a binding agent between the nanosized cathodic particles and the coating material. The cyclic performance and thermal stability of the coated $Li[Ni_{0.2}Li_{0.2}Mn_{0.6}]O_2$ nanoparticles are significantly enhanced, showing that the ZrO_2 coating layer successfully protected the nanoparticles from the reactive electrolyte.

1. Introduction

The cathode material is one of the key factors determining the capacity, cyclic performance and safety of lithium-ion batteries [1–4]. Due to its high voltage capacity, good cycling properties and easy preparation, lithium cobalt oxide ($LiCoO_2$) is a primary component of cathodes used in rechargeable lithium-ion batteries. However, in order to increase the energy density and decrease the cost and toxicity associated with lithium-ion batteries, many researchers have tried to find suitable substitutes for $LiCoO_2$ [5–9]. Li-rich layered oxides, such as solid solutions of layered Li_2MnO_3 and $LiMO_2$ (where M = Mn, Co, Ni, etc.), are promising new cathode materials for lithium-ion batteries owing to their high energy-storing capacities [10–18]. However, these materials face several major issues that need to be solved before commercialization can occur, including poor rate capability and cyclic performance.

A possible approach for enhancing the poor rate capability of cathodes is reducing the particle size. Nanometer-sized particles will decrease the diffusion distance of the electrons and lithium ions and increase the surface area. This, in turn, will facilitate the intercalation/deintercalation of the lithium ions [19–21]. A combustion method has been suggested as a cheap and simple method to fabricate nanosized Li-rich layered oxides [22–26]. However, in practice, the powders prepared by the combustion method form large aggregates instead [22,23]. Hence, the real size of the powder clusters, consisting of nanosized primary particles, reaches several micrometers. Our study was motivated by the fact that if the primary particles in these powder clusters could be successful

* Corresponding author. Tel.: +82 31 249 9769.
E-mail addresses: yjpark2006@kyonggi.ac.kr, yjparketri@yahoo.co.kr (Y.J. Park).

0378-7753/$ – see front matter © 2013 Elsevier B.V. All rights reserved.
http://dx.doi.org/10.1016/j.jpowsour.2013.01.154

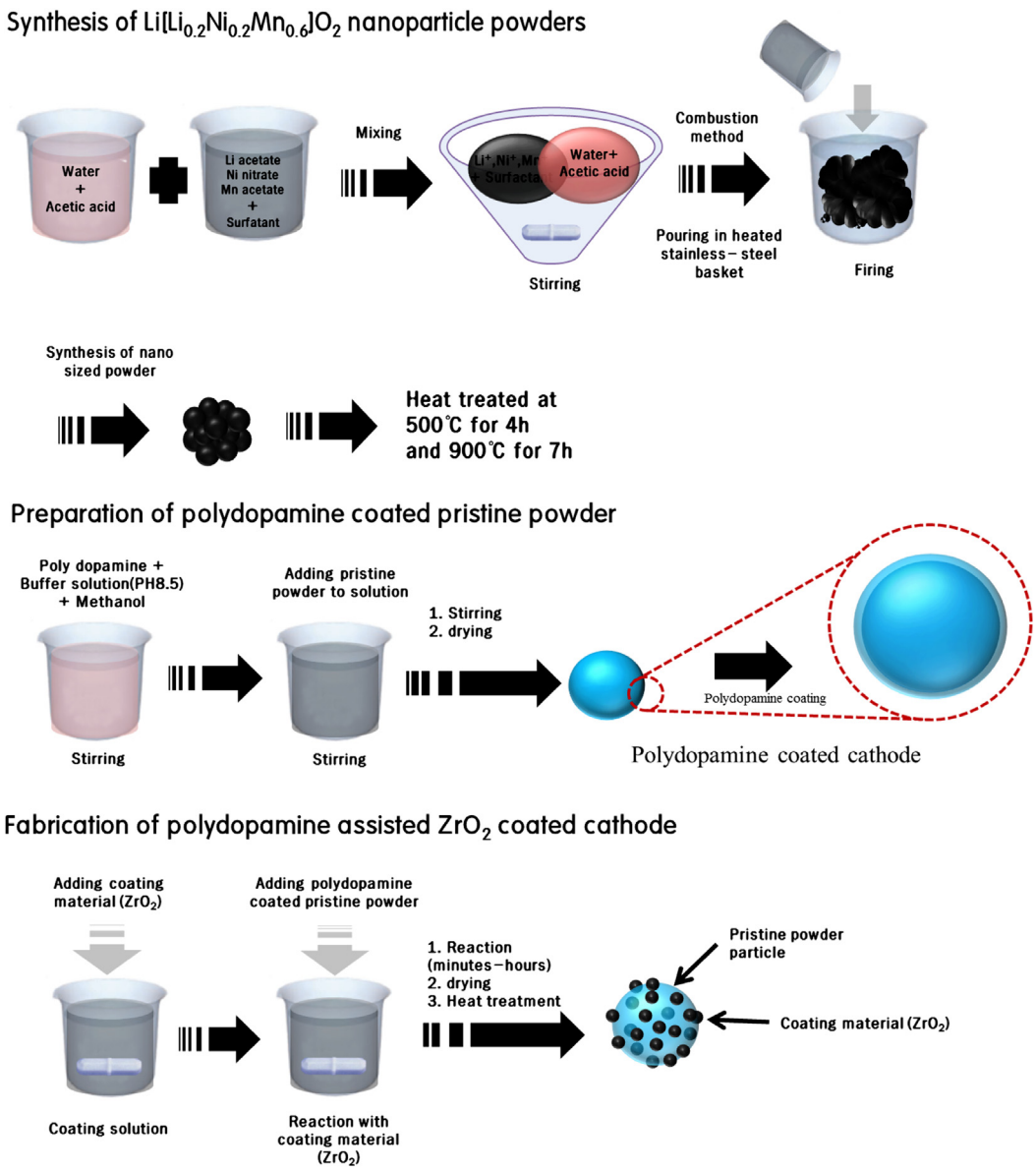

Fig. 1. Schematic diagram showing the procedure used for synthesizing $Li[Ni_{0.2}Li_{0.2}Mn_{0.6}]O_2$ nanoparticles using dispersing agents and the procedure used for forming polydopamine-assisted ZrO_2 coatings on the surface of pristine samples.

dispersed, the combustion method could be an easy and promising method for the fabrication of cathode powders whose particle is actually nanosized.

In the first part of our study, three kinds of dispersing agents (gelatin, urea, and Pluronic® P-123 (P123)) were introduced during the preparation of $Li[Ni_{0.2}Li_{0.2}Mn_{0.6}]O_2$ nanoparticles using the combustion method in order to prevent the primary nanoparticles from aggregating. These three dispersing agents are known to effective for fabricating cathodes containing nanocrystalline particles [27–30]. The dispersing agents are expected to act as dispersing agents and prevent the primary particles from aggregating during the combustion process.

Nanoparticle powders are advantageous as they have large surface areas, and this yields improvements in the rate capacities of the cathodes. However, there are several disadvantages including deterioration in the cyclic performance and poor thermal stability of the cathodes. The cyclic performance is mainly dependent on side reactions between the cathode and the electrolyte. The large surface areas of the nanoparticle containing cathodes may therefore lead to an increase in undesirable side reactions between with the cathode and the electrolyte; these include dissolution of transition metals and the formation of an interfacial layer. The increase in the electrolyte–electrode contact area may also lead to deterioration in the thermal stability of the cathodes, which is associated with side reactions. The surface of the cathodes can be modified by coating them with stable materials. This has been shown to be an effective method of preventing side reactions and protecting the cathodes from reactive electrolytes. It has been reported that coated cathodes exhibit significantly improved cyclic performances and thermal stabilities [17,31–35]. However, surface coating of cathodes, formed of nanoparticles, has been scarcely attempted due to the difficultly in dispersing the coating material homogeneously over the surface of the nanoparticles. To date, surface coating has mainly been carried out for cathodes formed of micrometer, or larger, particles with circular shapes.

In the next step of this study, $Li[Ni_{0.2}Li_{0.2}Mn_{0.6}]O_2$ nanoparticles, prepared by dispersing agent-assisted combustion, were coated in order to improve cyclic performance. Zirconium dioxide (ZrO_2),

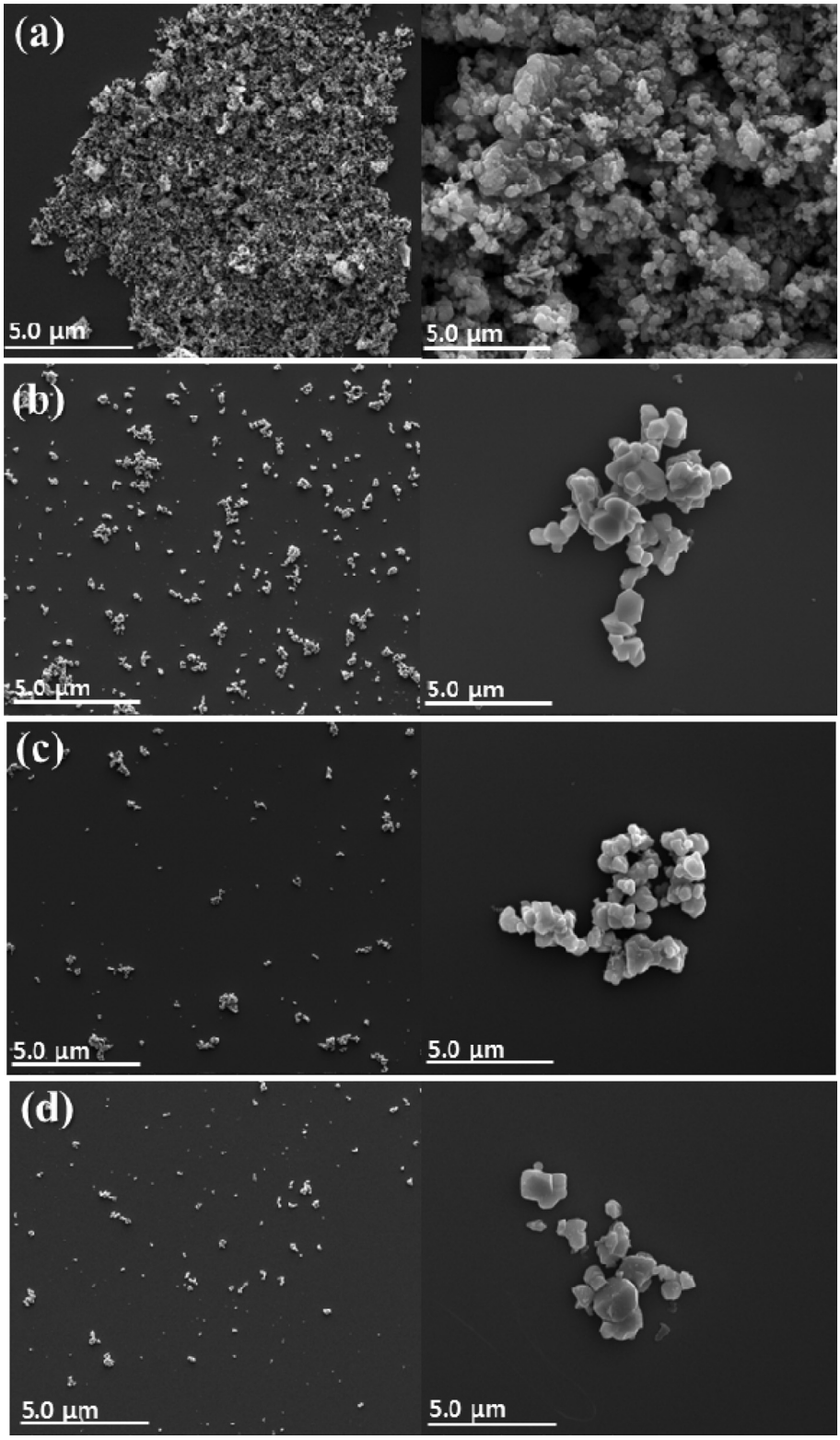

Fig. 2. SEM images of the $Li[Ni_{0.2}Li_{0.2}Mn_{0.6}]O_2$ nanoparticles. (a) Plain sample, (b) Gelatin sample, (c) Urea sample and (d) P123 sample.

a stable oxide, was used as the coating material. In order to apply the coating homogeneously to the surface of the nanoparticles, a layer of polydopamine, which acted as a binding assistant, was introduced. According to the literature, polydopamine can be used to modify a wide variety of material surfaces, making them extremely versatile platforms for secondary reactions [37–41]. Thus, a polydopamine layer coated on to the surface of the pristine cathode is expected to facilitate a reaction with the coating material. The ZrO_2-coated $Li[Ni_{0.2}Li_{0.2}Mn_{0.6}]O_2$ nanoparticles are expected to show not only good rate capability, which is

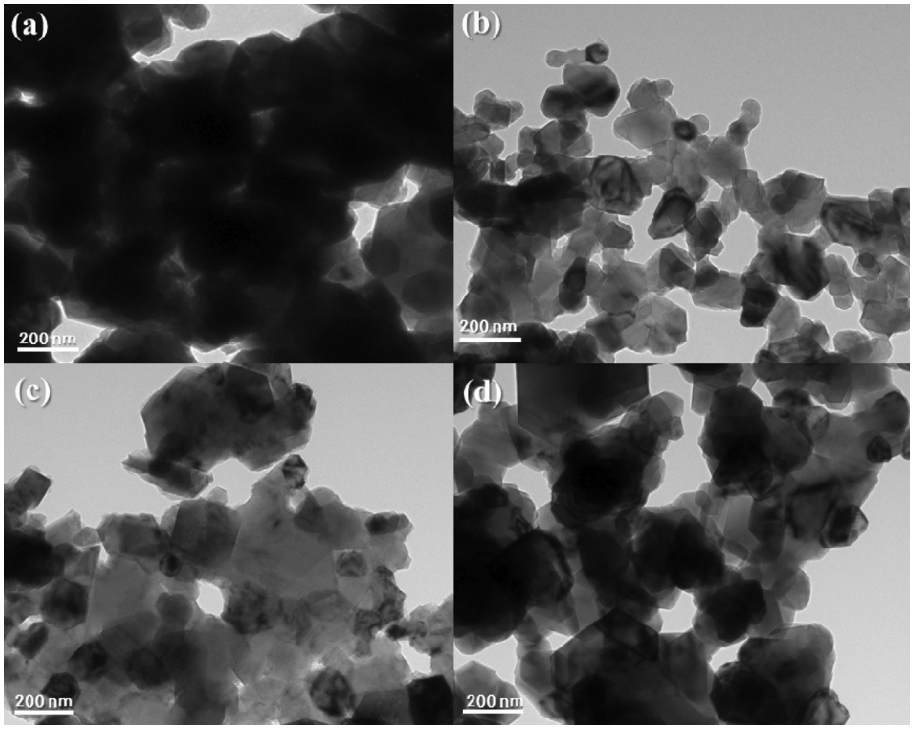

Fig. 3. TEM images of the $Li[Ni_{0.2}Li_{0.2}Mn_{0.6}]O_2$ nanoparticles. (a) Plain sample, (b) Gelatin sample, (c) Urea sample and (d) P123 sample.

advantageous for cathodes formed of nanoparticles, but also stable cyclic performance and improved thermal stability owing to the protective effect of the ZrO_2 layer.

2. Experimental

The $Li[Ni_{0.2}Li_{0.2}Mn_{0.6}]O_2$ nanoparticles were prepared using the combustion method. Dispersing agents were used to prevent aggregation of the nanoparticles. Manganese acetate tetrahydrate [$Mn(CH_3CO_2)_2{\cdot}4H_2O$ (Aldrich, 99+%)], nickel(II) nitrate hexahydrate [$Ni(NO_3)_2{\cdot}6H_2O$ (Aldrich, 99.99%)], lithium acetate dihydrate [$CH_3CO_2Li{\cdot}2H_2O$ (Aldrich, 98%)] were used as source materials. Three types of dispersing agents, gelatin (Aldrich), urea (Aldrich, 97%) and P123 (a (EO)20(PO)70(EO)20 triblock copolymer) (Aldrich), were added to control the size of the particles in the cathode powder. The source materials were dissolved in a solvent composed of distilled water and acetic acid, in the appropriate stoichiometric amounts, to form a solution. Approximately 5 g of dispersing agent was added, per 10 g of source material, to each solution. The solutions were continuously stirred on a hot plate at 80–90 °C. As the solvent evaporated the mixed solution turned into a viscous gel. The gel was annealed at 400 °C for 1 h. A vigorous decomposition process occurred resulting in the formation of an ash-like powder. The decomposed powder was ground and then annealed in air at 500 °C for 4 h and at 800 °C for 6 h. The powder was then quenched to room temperature. Four samples of nanoparticles were prepared in this manner; one without any dispersing agent, one with urea, one with P123 and one with gelatin. The samples are hereafter referred to as “Plain”, “Urea”, “P123”, and “Gelatin” respectively. The Brunauer–Emmett–Teller (BET) surface area of powder particles was obtained using a continuous-flow gas (N_2) adsorption apparatus (Micromeritics, ASAP 2020). The composition of the powder was measured by inductively coupled plasma optical emission spectrometry (ICP-OES) (PerkinElmer-OPTIMA 7300DV) (The typical composition of the powder was approximately $Li[Ni_{0.2}Li_{0.16}Mn_{0.64}]O_{1.95}$).

The surfaces of the $Li[Ni_{0.2}Li_{0.2}Mn_{0.6}]O_2$ nanoparticles were modified by applying a coating of ZrO_2 in order to enhance the cyclic performance and thermal stability of the cathode. A polydopamine layer was introduced to facilitate the reaction between the surface of pristine powder particles and the coating material. The Gelatin sample particles were selected as ‘pristine’ sample for coating as they were fine in size and had homogeneous sizes. The polydopamine layer was applied by immersing the Gelatin sample into a dopamine solution containing Tris-buffer solution (10 mM; pH 8.5) (Aldrich) and methanol (Aldrich, 99.9%) as cosolvents (CH_3OH:buffer = 1:1 by vol.). The mixture was mechanical stirred at room temperature for 30 min, until all the particles were suspended in the solution. The mixture solution was then centrifuged, washed with ethanol and distilled water several times, and dried at 90 °C for 24 h. To produce the ZrO_2 coating solution, zirconium(IV) oxynitrate hydrate [$N_2O_7Zr{\cdot}xH_2O$ (Aldrich, 99%)] was dissolved in ethanol at 25 °C for a period of 1 h, while being stirred continuously. The polydopamine-coated Gelatin sample was added to the ZrO_2 solution and stirred at 50 °C until all the ethanol had evaporated. The sample was then dried at 90 °C for 24 h and annealed at 400 °C for 3 h in air. Fig. 1 shows the scheme used for the synthesis of the $Li[Ni_{0.2}Li_{0.2}Mn_{0.6}]O_2$ nanoparticles using dispersing agents and the ZrO_2-coating process using a polydopamine layer.

The surface morphologies of the samples were observed using a field-emission scanning electron microscope (FE-SEM) (Nova Nano 200) and a transmission electron microscope (TEM) (AP tech TECNAI G2 F30 S-Twin) operating at 200 kV. Before measurement, the powder was dispersed and sonicated in the ethanol solution, and then dried to break soft-aggregation of the powder. A particle size analyzer (MICRO TRAC S3500) was used to confirm the particle sizes and their distribution. For electrochemical testing, a slurry was prepared by mixing carbon black (Super P) with polyvinylidene fluoride (PVDF) in a weight ratio of 80 (cathode powder):12 (super P):8 (PVDF). A coin-type cell (2032) compromising a cathode, a Li-metal anode, a separator and an electrolyte was used. The

electrolyte used was a 50:50 vol% mixture of $LiPF_6$ (1 M) and ethylene carbonate/dimethyl carbonate (EC/DMC). The cells were subjected to galvanostatic cycling using a WonATech voltammetry system. Thermal stability of the charged (4.8 V) electrode was analyzed by differential scanning calorimetry (DSC) (Mettler Toledo) using a high-pressure DSC pan.

3. Results and discussion

3.1. Characterization of $Li[Ni_{0.2}Li_{0.2}Mn_{0.6}]O_2$ nanoparticles

Fig. 2 shows the scanning electron microscopy (SEM) images of the $Li[Ni_{0.2}Li_{0.2}Mn_{0.6}]O_2$ powders prepared with and without dispersing agents. All the powders consist of primary particles smaller than 500 nm. However, the distribution and dispersion of the particles differs significantly for different fabrication conditions. The particles in the Plain sample show a high degree of aggregation (Fig. 2a), while the samples prepared using dispersing agents are well dispersed (Fig. 2b–d). Some of the dispersing agents-containing particles seem to be partially aggregated. However, the size of the particle clusters is much smaller than that of the Plain sample particle aggregates. The decrease in aggregation is due to the presence of the dispersing agents.

To investigate the size and shape of the different particles in detail a transmission electron microscopy (TEM)-study was performed (Fig. 3). The particles in the Plain sample are large in size and polydisperse due to the high degree of agglomeration of the primary particles. The samples prepared using dispersing agents, on the other hand, contain particles that are more uniform in size and that form smaller clusters. The Gelatin sample contains the smallest and most uniform particles.

The $Li[Ni_{0.2}Li_{0.2}Mn_{0.6}]O_2$ nanoparticles were measured using a particle-size analyzer. Fig. 4 shows the size distributions of the particles in the different samples. The cumulative values of the particle sizes are summarized in Table 1. The % and size values of Table 1 mean that cumulative % of the particles has smaller size than the designated size value on the right side. As an example, the Gelatin sample displays 70%: 0.139 μm and 90%: 0.493 μm. This means that 70% of the particles for Gelatin sample are smaller size than 0.139 μm and 90% of the particles are smaller size than 0.493 μm. The majority of the particles in the Plain sample are several micrometers in size. However, the SEM and TEM images show that the primary particles are much smaller. The large size measured using the particle-size analyzer results from significant aggregation of the primary particles. The samples prepared using dispersing agents have significantly reduced particle sizes. As observed in the SEM and TEM images, the Gelatin sample particles are the smallest and most homogeneously distributed of all the different samples, with 90% of the particles being approximately 0.5 μm in size. This indicates that Gelatin is a very effective dispersing agent for preparing $Li[Ni_{0.2}Li_{0.2}Mn_{0.6}]O_2$ nanoparticle powders. The presence of glycine residues in gelatin, makes it an excellent fuel for vigorous combustion reactions. Gelatin is also a good dispersing agent for sol–gel thermolysis processes owing to the long chain linkages in the amino acids it contains [29]. The Urea sample also contains small particles. Although a larger percentage of the particles are aggregated, the average size of the particles is ~0.7 μm, indicating that Urea can also be used as a fuel and dispersing agent in these combustion reactions. The P123 sample contains particles that are somewhat larger than those of both the

Table 1
Particle size distribution of the $Li[Ni_{0.2}Li_{0.2}Mn_{0.6}]O_2$ nanoparticle samples prepared with and without dispersing agents. The percentages denote the cumulative values of the particle sizes.

Plain sample		Gelatin sample		Urea sample		P123 sample	
%Tile	Size (μm)	%Tile	Size (μm)	%Tile	Size (μm)	%Tile	Size (μm)
10	1.328	10	0.098	10	0.134	10	0.195
30	3.25	30	0.116	30	0.156	30	0.355
50	5.08	50	0.129	50	0.174	50	0.575
70	7.87	70	0.139	70	0.201	70	1.257
90	16.0	90	0.493	90	0.738	90	2.938

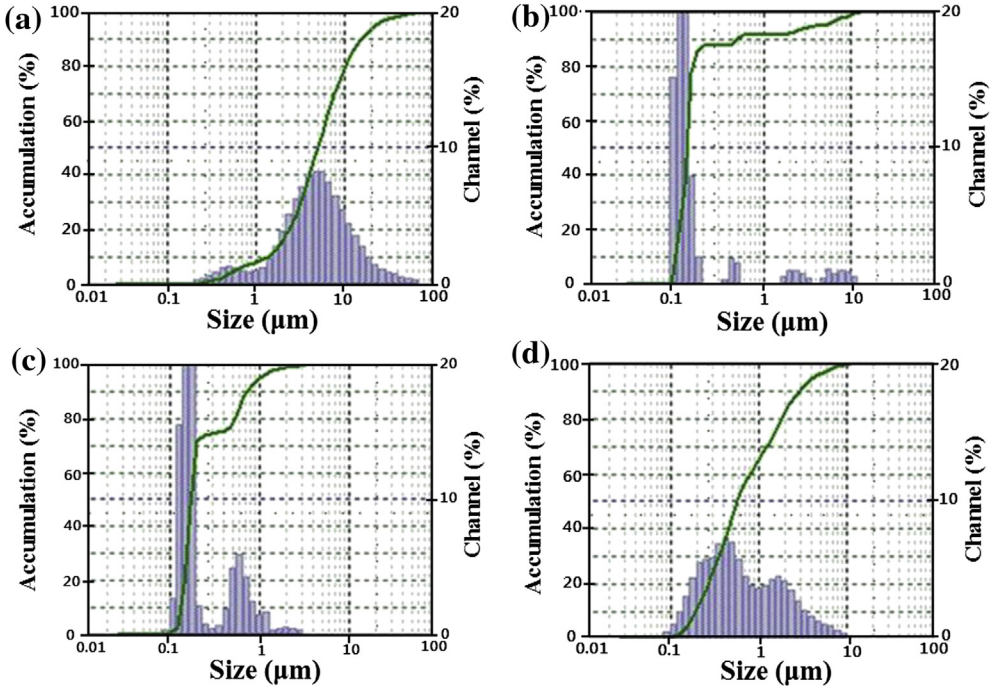

Fig. 4. Size distribution of the $Li[Ni_{0.2}Li_{0.2}Mn_{0.6}]O_2$ nanoparticles. (a) Plain sample, (b) Gelatin sample, (c) Urea sample and (d) P123 sample.

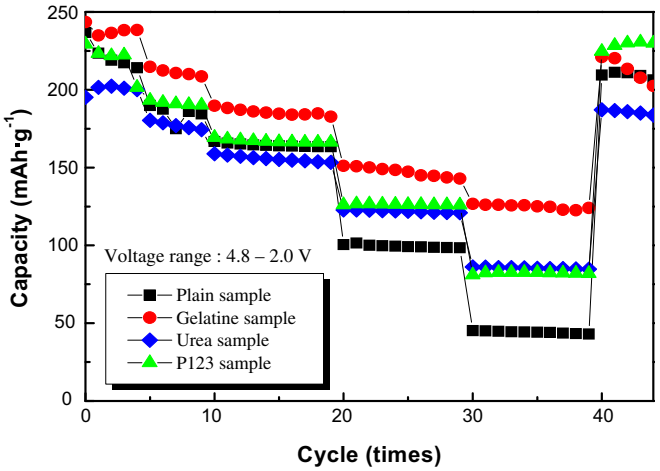

Fig. 5. The discharge capacities of $Li[Ni_{0.2}Li_{0.2}Mn_{0.6}]O_2$ nanoparticle samples prepared with and without dispersing agents measured at current densities of 40 (1–5 cycles and 41–45 cycles), 100 (6–10 cycles), 200 (11–20 cycles), 600 (21–30 cycles), and 1200 mA g^{-1} (31–40 cycles) at voltages ranging from 2.0 to 4.8 V.

Gelatin and Urea samples, but smaller than the Plain sample. P123 is a typical nonionic dispersing agent usually used as a structure-directing agent for synthesizing ordered mesoporous materials [27,30]. Although P123 is favorable for the formation of mesoporous materials, it appears not to be suitable for dispersing primary particles in combustion reactions.

To investigate the effects of dispersing agent on the capacity and rate capability, the electrochemical properties of the $Li[Ni_{0.2}Li_{0.2}Mn_{0.6}]O_2$ nanoparticle powders were characterized. Fig. 5 shows the discharge capacities of the samples measured at current densities of 40, 100, 200, 600 and 1200 mA g^{-1} for voltages ranging from 2.0 to 4.8 V. The discharge capacities of the Plain and P123 samples are similar for current densities between 40 and 200 mA g^{-1}. However, at higher current densities (600 and 1200 mA g^{-1}), the P123 sample has a higher discharge capacity than the Plain sample. Moreover, at current density of 40 mA g^{-1} after 40th cycles, the high capacity over 230 mAh g^{-1} was returned, which indicates the stable cyclic performance of the P123 sample. This result may be associated with not only reduced particle size but also high porosity of the P123 samples. At current densities of 40 and 100 mA g^{-1}, the discharge capacity of the Urea sample is a little lower than that of the Plain sample. It could not exclude the possibility that Urea sample has relatively low phase integrity, i.e., some oxygen loss of the phase could be occurred due to the combustion process of the Urea. This could lead to some differences in the reaction mechanism on charge-and discharge process [43], and reduce the capacity of the cell. However, the Urea sample has a higher discharge capacity at higher current densities (600 and 1200 mA g^{-1}), indicating an improvement in the rate capability. The effect of the particle size on the rate capability can be clearly observed for the Gelatin sample, which has discharge capacity and rate capability that are considerably superior to those of the Plain sample (Fig. 5).

Fig. 6 shows the voltage profiles of the samples at current densities of 40, 200, and 1200 mA g^{-1}. The discharge capacity of the gelatin sample is approximately 243 mAh g^{-1}, which is higher than the discharge capacities measured for any of the other samples at all current densities. Moreover, at a current density of 1200 mA g^{-1}, the capacity retention of the Gelatin sample is approximately 52% of the capacity measured for a current density of 40 mA g^{-1}. At 1200 mA g^{-1}, the Urea and P123 samples have capacity retentions of approximately 44% and 35% of the capacity at 40 mA g^{-1}, respectively. However, the capacity retention of the Plain sample is only 17% for the same conditions. Table 2 summarizes the discharge capacities and capacity retentions of the samples at the different current densities. The values were measured at the first cycle for

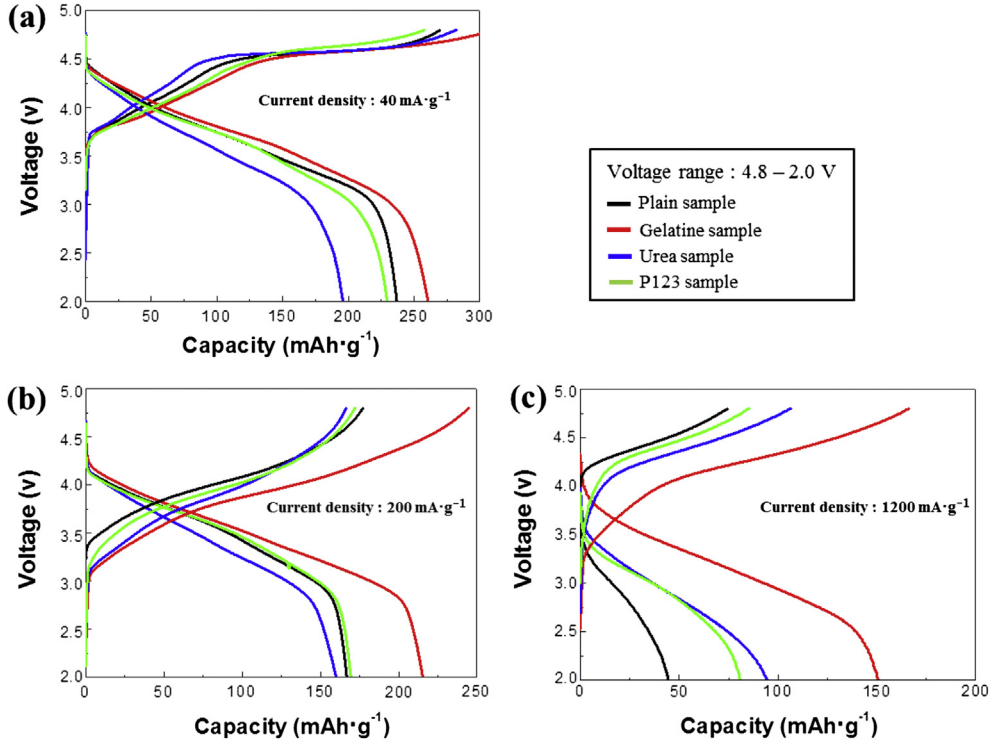

Fig. 6. The voltage profiles, measured at various current densities, of the $Li[Ni_{0.2}Li_{0.2}Mn_{0.6}]O_2$ nanoparticle samples prepared with and without dispersing agents. (a) 40 mA g^{-1} (initial cycle of Fig. 5), (b) 200 mA g^{-1} (11th cycle of Fig. 5) and (c) 1200 mA g^{-1} (31st cycle of Fig. 5).

Table 2
Discharge capacity and capacity retention of the $Li[Ni_{0.2}Li_{0.2}Mn_{0.6}]O_2$ nanoparticle samples at various current densities. The values shown are for the initial cycles at each current density.

	Plain sample (mAh g^{-1})	(%)	Gelatin sample (mAh g^{-1})	(%)	Urea sample (mAh g^{-1})	(%)	P123 sample (mAh g^{-1})	(%)
40 mA g^{-1}	236.8	100	243.6	100	195.1	100	229.4	100
100 mA g^{-1}	189.8	80.1	214.8	88.2	180.3	92.4	201.5	87.8
200 mA g^{-1}	166.7	70.4	189.7	77.9	158.9	81.4	169.4	73.8
600 mA g^{-1}	100.5	42.4	151.1	62.0	122.8	62.9	126.1	54.9
1200 mA g^{-1}	45.2	16.9	126.7	52.0	86.2	44.1	81	35.3

each current density. The enhanced rate capability of samples prepared using dispersing agents can be attributed to the reduction in the particle sizes and the concomitant increase in the surface areas (the surface area of the Gelatin sample was 17.41 m^2 g^{-1}, while the surface area of the Plain sample was just 3.02 m^2 g^{-1}). The reduction in the particle sizes may increase the rate of lithium insertion/removal and electron transport owing to the shorter transport distances. A larger contact area between the electrode

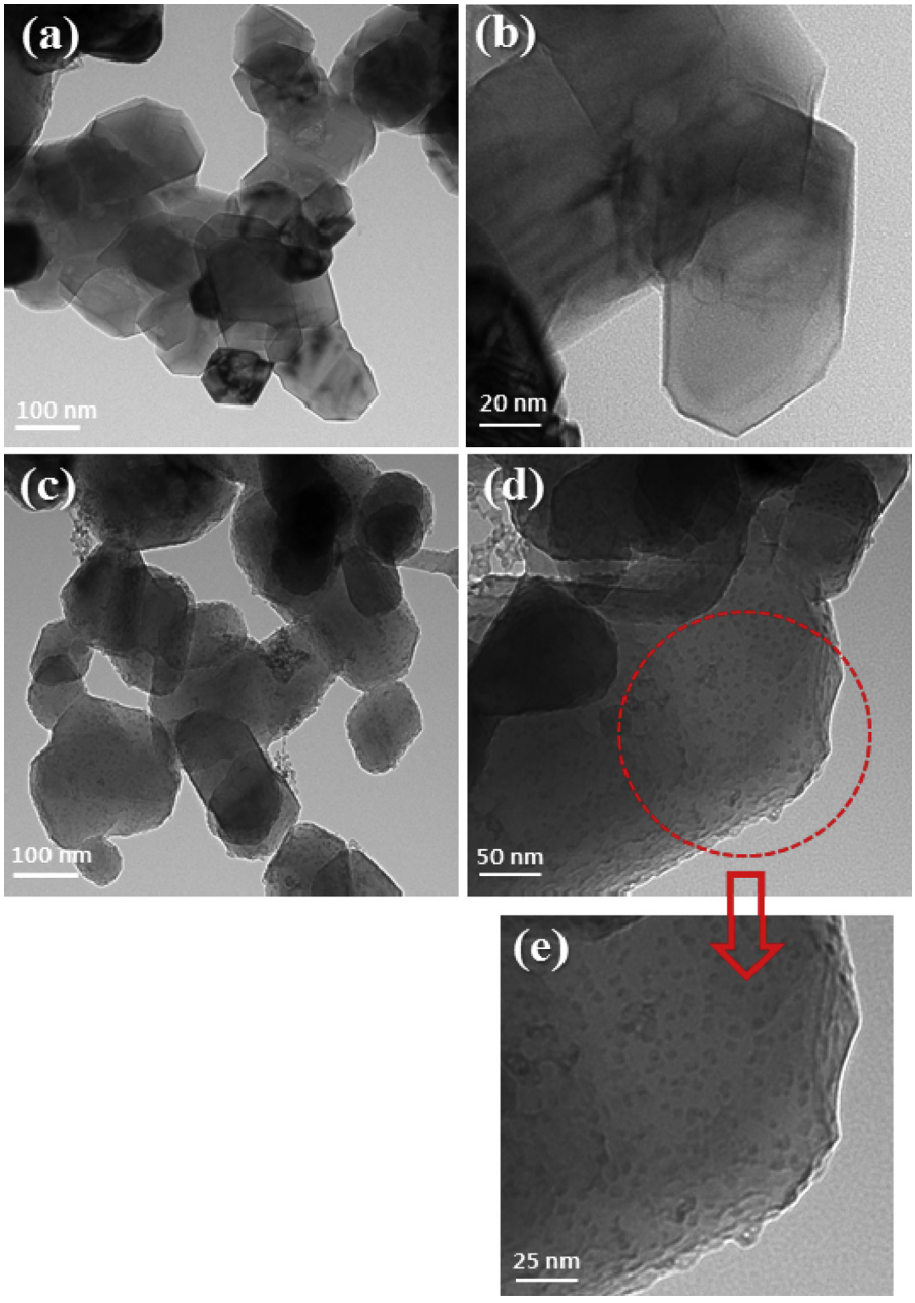

Fig. 7. TEM images of the (a, b) pristine (uncoated) and (c–e) ZrO_2-coated Gelatin samples.

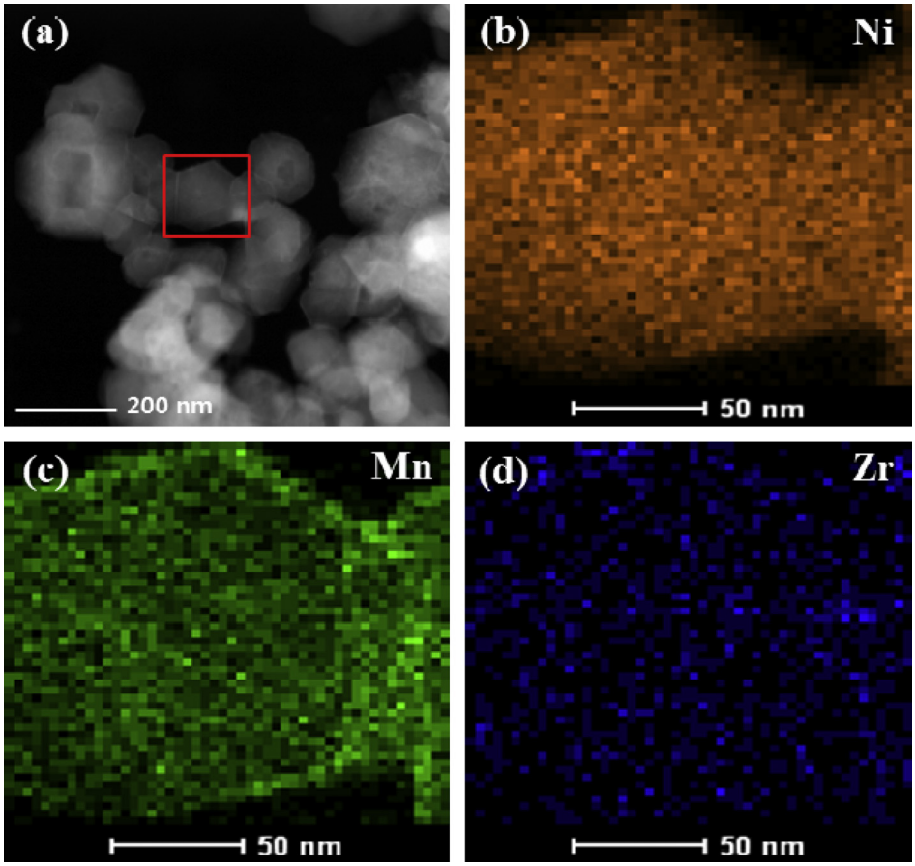

Fig. 8. Elemental mapping of a ZrO_2 coated Gelatin sample using TEM–EDS. (a) TEM image showing the area analyzed (denoted by the red square). EDS maps of (b) Ni, (c) Mn and (d) Zr. (For interpretation of the references to color in this figure legend, the reader is referred to the web version of this article.)

and electrolyte should also facilitate the intercalation/deintercalation of the lithium ions across the interface. The Gelatin sample, which has the smallest average particle size and size distribution, exhibits the advantages of particle size reduction most clearly.

3.2. Surface coating of $Li[Ni_{0.2}Li_{0.2}Mn_{0.6}]O_2$ nanoparticles mediated by polydopamine

As a following work, the surface of $Li[Ni_{0.2}Li_{0.2}Mn_{0.6}]O_2$ nanoparticles was modified with stable ZrO_2 to prevent unwanted side reactions, which is expected to severely be occurred due to their wide surface area. A point to be considered is that the pristine (uncoated) powders were very small in size (0.1–0.5 μm) and had various shapes, i.e., they were not circular-shapes like the particles of powders fabricated by coprecipitation methods. Surface-coating techniques have been successfully adopted for the modification of microscale-sized cathodic powders with circular shapes. However, as the sizes of the particles of the powders reduce further, it becomes difficult to homogeneously coat the surfaces of the powder particles. Moreover, if the powders are not circular shaped but have various other structures, the coating particles cannot be dispersed homogeneously owing to the different surface energies of the uncoated powder particles.

In order to overcome this problem, polydopamine was used as a special binding agent. The binding nature of polydopamine was discovered during the analysis of the special adhesive proteins found in mussels. Mussels have been known to very strongly attach to all types of inorganic and organic surfaces. It has been reported that the adhesive ability of the mussels lies in the amino-acid composition of the proteins they contain. These proteins are rich in 3,4-dihydroxy-L-phenylalanine (DOPA) and lysine amino acids [36,37]. On the basis of these findings, Lee et al. suggested that a polydopamine coating functionalized with DOPA and lysine side-chains could be used as an effective binding agent [36,37]. A polydopamine layer can be used to modify the surface of the cathode to create a reactive platform facilitating the reaction with ZrO_2. The binding properties of polydopamine were tested using the $Li[Ni_{0.2}Li_{0.2}Mn_{0.6}]O_2$ nanoparticles prepared using gelatin.

Fig. 7 shows the TEM images of the pristine (uncoated) and ZrO_2-coated Gelatin sample. The surface of the pristine powders is smooth and do not contain heterophase particles. The coated powders are covered with a nano-layer of the coating material. Fig. 7c and d shows the ZrO_2-coated Gelatin sample. The coating particles (ZrO_2) are homogeneously distributed and well dispersed over the surfaces of the Gelatin sample. The sizes of the ZrO_2 particles of the coating material are less than 5 nm. Fig. 8 shows the elemental mapping results obtained by TEM-energy dispersive X-ray spectrometry (EDS). The red square in Fig. 8a shows the analyzed area. Fig. 8b–d shows the EDS maps for Ni and Mn and Zr, respectively. The intensity of the pixels indicates the concentration of the respective element. Ni, Mn and Zr are all uniformly distributed over the analyzed area indicating that the nanoparticles are homogeneously coated with ZrO_2.

To confirm the effectiveness of using the polydopamine layer, a 'control' ZrO_2-coated Gelatin sample was fabricated using the

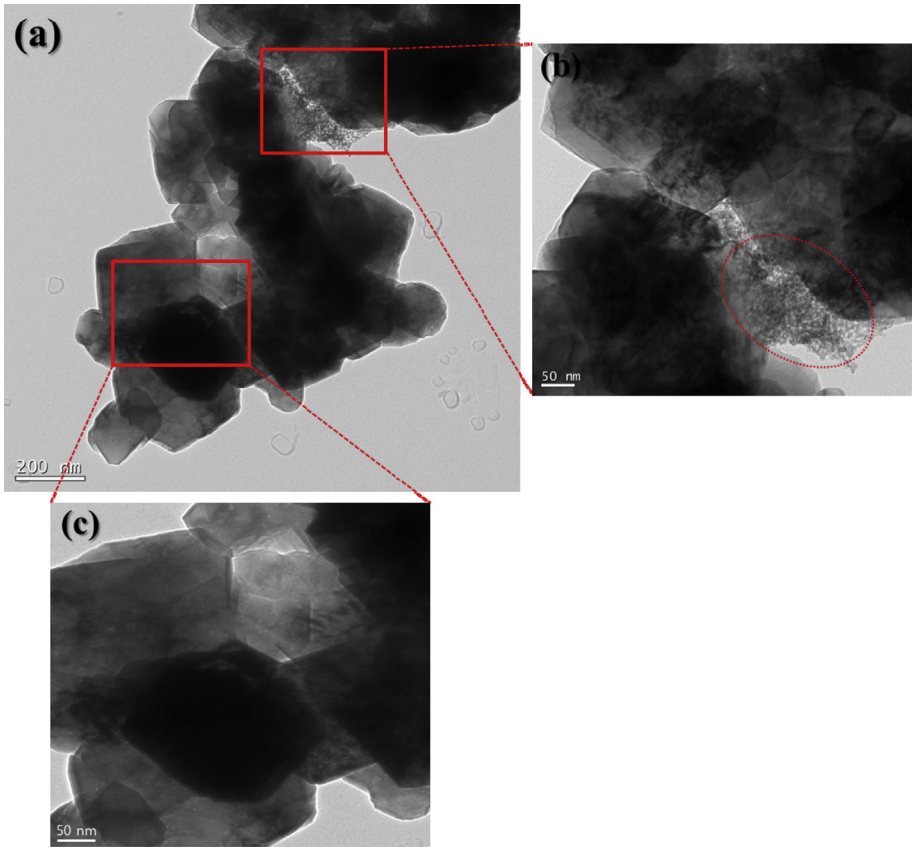

Fig. 9. TEM image of the (a) polydopamine-free ZrO_2 coated Gelatin sample and (b, c) magnified TEM images of marked points by red square. (For interpretation of the references to color in this figure legend, the reader is referred to the web version of this article.)

same protocol as in Fig. 1 (bottom side), but without the polydopamine. Fig. 9 shows the TEM images of the polydopamine-free ZrO_2 coated $Li[Ni_{0.2}Li_{0.2}Mn_{0.6}]O_2$ powders. Unlike the polydopamine-assisted sample, the polydopamine-free coated powder showed that the ZrO_2 particles seemed to be severely aggregated on the surface of the pristine powder (Fig. 9b). Moreover, most of the surface of the powders was clean without attached coating material, as shown in Fig. 9c. In these images suggest that the ZrO_2 coating layer did not homogeneously react on the surface of the pristine powder, and they simply aggregated and crystallized upon the heating process. The results in Figs. 7–9 show that polydopamine is very effective in binding ZrO_2 to the surface of pristine Gelatin powder. Successfully coating a layer of polydopamine on the surfaces of pristine powder assists not only the adhesion, but also the homogeneous dispersion of the ZrO_2 coating material. This new and facile method can be applied to various coating processes for nanoparticle powders.

To examine the effects of the polydopamine-assisted ZrO_2 coatings on the capacity, rate capability and cyclic performance, the electrochemical properties of the coated and pristine (uncoated) Gelatin samples were characterized. The samples were cycled at current densities of 40, 100, 200, 600, and 1200 mA g^{-1} at voltages between 2.0 and 4.8 V. Five cycles were performed at each current density. Fig. 10 shows the discharge profiles of the samples at each current density, where the value given is for the second cycle after the initial irreversible charge–discharge process. The discharge capacity of the coated samples seems to be a little bit decreased compared to that of the uncoated Gelatin sample. Some possible factors such as slightly increased overall weight of the electrode material, low electronic conductivity due to coating layer, and residual carbon originated from polydopamine layer could lead to deterioration of capacity. However, the capacity of coated sample was still higher than those of other samples (not only the Plain sample but also the Urea and P123 samples).

Surface coatings are expected to enhance cyclic performances because of their protective effects. Fig. 11a shows the cyclic performances of the Plain, Gelatin and ZrO_2 coated Gelatin samples. Initially, the cells were cycled twice at a current density of 40 mA g^{-1} to allow a slow initial irreversible reaction. The cells were then cycled fifty times at a current density of 100 mA g^{-1}. During the initial charging process, $Li[Ni_{0.2}Li_{0.2}Mn_{0.6}]O_2$ has a long plateau in the capacity for voltages above 4.4 V. This is attributed to removal of lithium accompanied by irreversible oxygen loss from the cathode. During this phase, oxygen loss can result in damage to the surface of the cathode leading to the deterioration of its cyclic performance. Slow initial cycles may result in a slower oxygen removal during the initial irreversible reaction, reducing the surface damage.

The discharge capacity of the Plain sample gradually decreases on cycling, at room temperature (30 °C), after the initial deviation (Fig. 11a). The poor cyclic performance is the one of the major problems that needs to be resolved before Li-rich layered oxides such as $Li[Ni_{0.2}Li_{0.2}Mn_{0.6}]O_2$ can be commercialized. It has been reported that oxygen loss from the surface of cathodic particles, during the initial charge process, is the main reason for inferior cyclic performance in Li-rich layered oxide cathodes [42]. The Gelatin sample exhibits a higher discharge capacity than the Plain sample due to the reduced particle size. However, on cycling, its capacity decreases more steeply than that of the Plain sample, which has larger particles. This deterioration of the cyclic

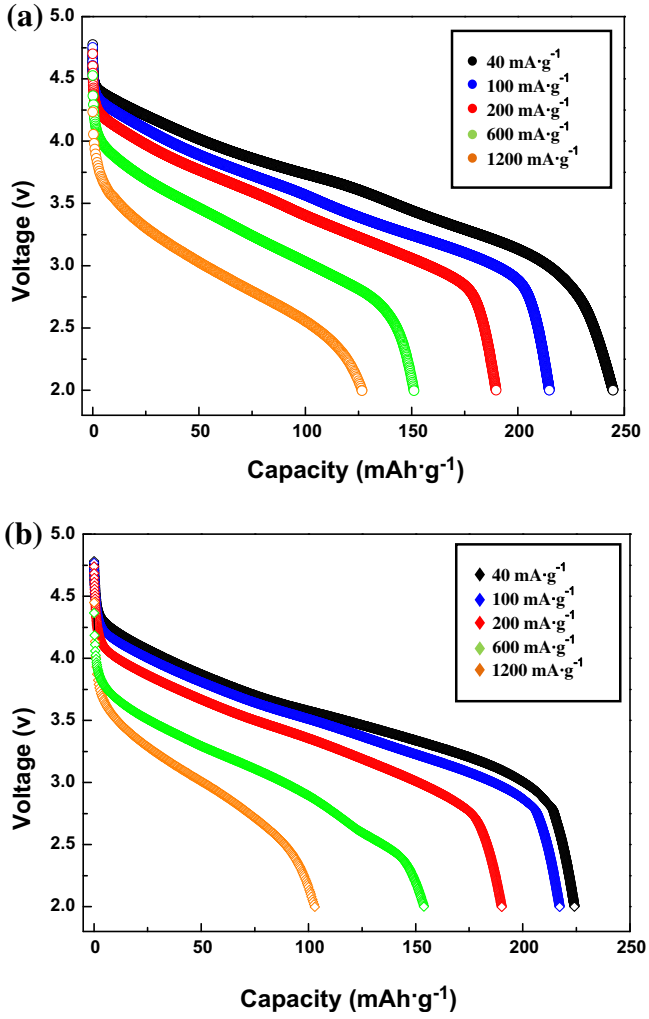

Fig. 10. The discharge profile of the pristine (uncoated) and ZrO_2 coated Gelatin samples at current densities of 40, 100, 200, 600, and 1200 mA g^{-1} at voltages ranging from 2.0 to 4.8 V. (a) Pristine Gelatin sample and (b) ZrO_2 coated Gelatin sample.

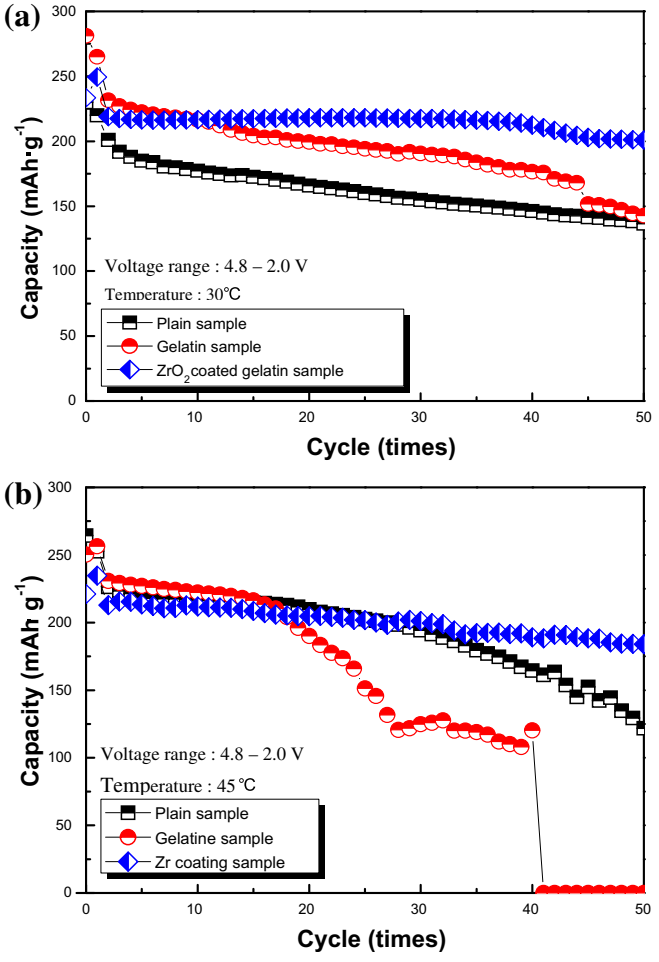

Fig. 11. Cyclic performance of the pristine (uncoated) and ZrO_2 coated Gelatin samples at voltages ranging from 2.0 to 4.8 V measured at (a) 30 °C and (b) 45 °C (the initial 2 cycles were measured at 40 mA g^{-1}, then cycled 100 mA g^{-1} until 50 cycles).

performance in nanoparticle cathodic materials is generally considered to originate from more active side reactions with the electrolyte. The small size of the Gelatin sample particles increases the surface area leading to a greater electrolyte/electrode contact area during cycling. The increase in the contact area with the electrolyte results in vigorous side reactions. As a result, nanoparticle cathodic powders are vulnerable to reactive electrolytes, which can cause deterioration in the cyclic performance.

As expected, the cyclic performance of the Gelatin sample is observed to be enhanced by the polydopamine-assisted ZrO_2 coating (Fig. 11a). More than 91% of the capacity (at third cycle) of the Gelatin sample was stably maintained over fifty cycles. The pristine Gelatin sample, on the other hand, is seen to retain only 62% of the capacity over the same number of cycles. This implies that the coating layer successfully suppresses side reactions with the electrolyte during cycling. Stable surface coatings can reduce the direct contact area between the cathode and electrolyte, protecting the cathode surface from reactive electrolytes [17,31–35]. The coating material may also be acting sacrifice electrode to prevent the damage of the pristine cathode. Cathodes based on Li-rich layered oxides, such as $Li[Ni_{0.2}Li_{0.2}Mn_{0.6}]O_2$, undergo surface damage due to oxygen loss during the initial charge process. A surface coating is therefore an effective method to protect vulnerable cathode surfaces and prevent side reactions. To further investigate the effectiveness of the polydopamine-assisted ZrO_2 coatings, cycling testing at high temperatures was performed. Fig. 11b shows the cyclic performance of the Plain, pristine Gelatin and ZrO_2 coated Gelatin samples at 45 °C for voltages ranging from 2.0 to 4.8 V. The side reactions between the electrolyte and cathode should increase at higher temperatures. It was therefore expected that the samples would undergo significant degradations in their cyclic performances. The capacity of the Plain sample is observed to significantly decrease on cycling at 45 °C. After fifty cycles the capacity retention of the Plain sample is only 54% of the capacity during the third cycle. For the Gelatin sample the discharge capacity drops rapidly to almost zero after forty cycles. This severe deterioration in cyclic performance is attributed to active side reactions originating from the large contact area between the electrode and electrolyte. In contrast, the ZrO_2 coated Gelatin sample exhibits a much better cyclic performance at 45 °C. Over 86% of the capacity at the third cycle is maintained after fifty cycles. This result confirms the fact that the polydopamine-assisted ZrO_2 coating layer is effective in protecting the surface of $Li[Ni_{0.2}Li_{0.2}Mn_{0.6}]O_2$ nanoparticle cathodes. Table 3 summarizes the discharge capacities and capacity retentions of the samples at the third and fiftieth cycles.

The thermal stability of $Li[Ni_{0.2}Li_{0.2}Mn_{0.6}]O_2$ nanoparticle electrodes, before and after coating, was investigated via DSC. The

Table 3
Discharge capacity measured at the third and fiftieth cycle for the Plain, pristine Gelatin and ZrO_2 coated Gelatin samples at 30 °C and 45 °C. The percentages refer to the retention of the capacity at third cycle after the fiftieth cycle.

Cycle	Plain sample (mAh g^{-1})	(%)	Gelatin sample (mAh g^{-1})	(%)	ZrO2 coated gelatin sample (mAh g^{-1})	(%)
3rd (30 °C)	201.0	100	231.6	100	218.9	100
50th (30 °C)	138.3	68.8	144.5	62.4	200.6	91.6
3rd (45 °C)	226.5	100	230.7	100	212.8	100
50th (45 °C)	121.7	53.7	0	0	184.2	86.6

samples were charged to 4.8 V prior to testing and sealed in a high-pressure DSC pan with 4 mg of electrolyte. Fig. 12 shows the DSC profiles of the pristine and ZrO_2 coated Gelatin samples. The pristine Gelatin sample (uncoated) and the electrolyte react thermally at approximately 170 °C. Heat is generated between 170 °C and 220 °C from the reaction (Fig. 12a). The total heat generated in the exothermic region is 188.8 J g^{-1}. For the ZrO_2 coated Gelatin sample, the exothermic region occurs between 190 °C and 231 °C and the heat generation sharply decreases to 96.04 J g^{-1} (Fig. 12b). This result confirms that the thermal stability of $Li[Ni_{0.2}Li_{0.2}Mn_{0.6}]O_2$ nanoparticle electrode is improved by the addition of the polydopamine-assisted ZrO_2 coating due to the protective effect of the coating layer.

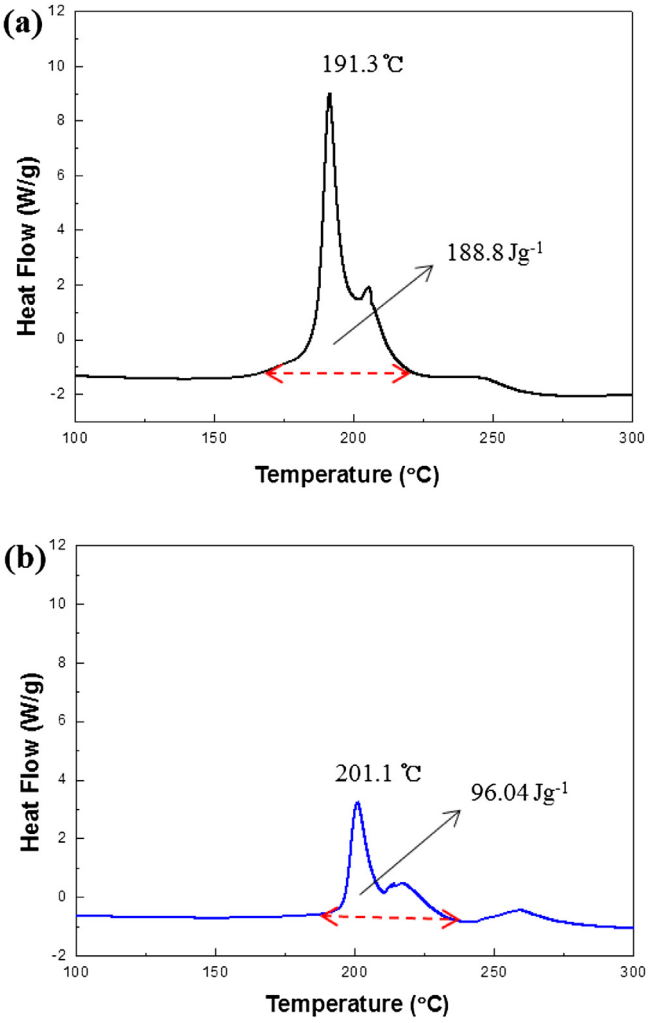

Fig. 12. DSC scans of fully charged pristine (uncoated) and ZrO_2 coated Gelatin samples (cut-off voltage is 4.8 V). (a) Pristine Gelatin sample and (b) ZrO_2 coated Gelatin sample.

4. Conclusions

$Li[Ni_{0.2}Li_{0.2}Mn_{0.6}]O_2$ nanoparticle powders were successfully synthesized using a dispersing agent-assisted combustion method. Three types of dispersing agents were introduced to disperse the primary particles and reduce the size of the $Li[Ni_{0.2}Li_{0.2}Mn_{0.6}]O_2$ nanoparticle powders. Gelatin was the most effective dispersing agent for both dispersing the primary particles and forming homogeneous particles with a reduced size. The $Li[Ni_{0.2}Li_{0.2}Mn_{0.6}]O_2$ nanoparticles prepared using dispersing agents had better rate capabilities than those containing no dispersing agents (Plain sample). This was due to the reduction in particle size, which shortened the transport distance, increasing the rate of lithium insertion/removal and improving the electronic conductivity. Polydopamine, in the form of a precoated layer, was successfully used as a binding agent for coating the surfaces of the $Li[Ni_{0.2}Li_{0.2}Mn_{0.6}]O_2$ nanoparticles with ZrO_2. The high reactivity of the polydopamine layer not only aided the adhesion of the ZrO_2 coating, but also helped in its homogeneous dispersion. The surfaces of ZrO_2 coated Gelatin sample particles were homogeneously covered with a layer containing 5 nm ZrO_2 particles. The polydopamine-assisted ZrO_2 coating was effective in improving the cyclic performance and thermal stability of a coated Gelatin sample. This suggests that the ZrO_2 coating suppressed side reactions with the electrolyte and protected the surface of $Li[Ni_{0.2}Li_{0.2}Mn_{0.6}]O_2$-based cathode.

Acknowledgment

This research was supported by the Converging Research Program through the Korean Ministry of Education, Science and Technology (2012K001263).

References

[1] J.B. Goodenough, J. Power Sources 174 (2007) 996.
[2] B. Scrosati, J. Garche, J. Power Sources 195 (2010) 2419.
[3] H.G. Song, J.Y. Kim, K.T. Kim, Y.J. Park, J. Power Sources 196 (2011) 6847.
[4] P. Gao, G. Yang, H. Liu, L. Wang, H. Zhou, Solid State Ion. 207 (2012) 50.
[5] N. Yabuuchi, Y. Makimura, T. Ohzuku, J. Electrochem. Soc. 154 (2007) A314.
[6] H.J. Lee, K.S. Park, Y.J. Park, J. Power Sources 195 (2010) 6122.
[7] J.W. Fergus, J. Power Sources 195 (2010) 939.
[8] J. Choi, A. Manthiram, J. Electrochem. Soc. 152 (2005) A1714.
[9] H.G. Song, J.Y. Kim, Y.J. Park, Electrochim. Acta 56 (2011) 6896.
[10] M.M. Thackeray, S.H. Kang, C.S. Johnson, J.T. Vaughey, R. Benedek, S.A. Hackney, J. Mater. Chem. 17 (2007) 12.
[11] T.A. Arunkumar, E. Alvarez, A. Manthiram, J. Mater. Chem. 18 (2008) 190.
[12] J. Gao, A. Manthiram, J. Power Sources 191 (2009) 644.
[13] X.J. Guo, Y.X. Li, M. Zheng, J.M. Zheng, J. Li, Z.L. Gong, Y. Yang, J. Power Sources 184 (2008) 414.
[14] J.H. Ryu, B.G. Park, S.B. Kim, Y.J. Park, J. Appl. Electrochem. 39 (2009) 1059.
[15] S.K. Martha, J. Nanda, G.M. Veith, N.J. Dudney, J. Power Sources 199 (2012) 220.
[16] J.H. Jeong, B.S. Jin, W.S. Kim, G. Wang, H.S. Kim, J. Power Sources 196 (2011) 3439.
[17] S.H. Kang, M.M. Thackeray, Electrochem. Commun. 11 (2009) 748.
[18] J. Li, R. Klöpsch, M.C. Stan, S. Nowak, M. Kunze, M. Winter, S. Passerini, J. Power Sources 196 (2011) 4821.
[19] Y.G. Guo, J.S. Hu, L.J. Wan, Adv. Mater. 20 (2008) 2878.
[20] P.G. Bruce, B. Scrosati, J.M. Tarascon, Angew. Chem. Int. Ed. 47 (2008) 2930.
[21] Y. Wang, G. Cao, Adv. Mater. 20 (2008) 2251.
[22] J.H. Ju, S.W. Cho, S.G. Hwang, S.R. Yun, Y. Lee, H.M. Jeong, M.J. Hwang, K.M. Kim, K.S. Ryu, Electrochim. Acta 56 (2011) 8791.

[23] Y.S. Hong, Y.J. Park, K.S. Ryu, S.H. Chang, M.G. Kim, J. Mater. Chem. 14 (2004) 1424.
[24] Z. Lu, J.R. Dahn, J. Electrochem. Soc. 149 (2002) A1454.
[25] Z. Lu, J.R. Dahn, J. Electrochem. Soc. 149 (2002) A815.
[26] Y.J. Park, Y.S. Hong, X. Wu, K.S. Ryu, S.H. Chang, J. Power Sources 129 (2004) 288.
[27] J. Wang, J. Zhou, Z. Li, Y. He, S. Lin, Q. Liu, M. Zhang, Z. Jiang, J. Solid State Chem. 183 (2010) 2511.
[28] C.Z. Lu, G.T.K. Fey, J. Phys. Chem. Solids 67 (2006) 756.
[29] A. Subramania, N. Angayarkanni, S.N. Karthick, T. Vasudevan, Mater. Lett. 60 (2006) 3023.
[30] Q. Wu, W. Li, Y. Cheng, Z. Jiang, Mater. Chem. Phys. 91 (2005) 463.
[31] J. Cho, Y.W. Kim, B. Kim, J. Lee, B. Park, Angew. Chem. Int. Ed. 115 (2003) 1618.
[32] J. Liu, A. Manthiram, J. Electrochem. Soc. 156 (2009) A833.
[33] S.T. Myung, K. Izumi, S. Komaba, Y.K. Sun, H. Yashiro, N. Kumagai, Chem. Mater. 17 (2005) 3695.
[34] S.H. Yun, K.S. Park, Y.J. Park, J. Power Sources 195 (2010) 6108.
[35] D.J. Lee, K.S. Lee, S.T. Myung, H. Yashirob, Y.K. Sun, J. Power Sources 196 (2011) 1353.
[36] H. Lee, B.P. Lee, P.B. Messersmith, Nature 448 (2007) 338.
[37] H. Lee, S.M. Dellatore, W.M. Miller, P.B. Messersmith, Science 318 (2007) 426.
[38] S.W. Taylor, D.B. Chase, M.H. Emptage, M.J. Nelson, J.H. Waite, Inorg. Chem. 35 (1996) 7572.
[39] N. Holten-Anderson, T.E. Mates, M.S. Toprak, G.D. Stucky, F.W. Zok, J.H. Waite, Langmuir 25 (2009) 3323.
[40] W.M. Chirdon, W.J. O'Brian, R.E. Robertson, J. Biomed. Mater. Res. Part B 532 (2003) 66B.
[41] J. Ryu, S.H. Ku, H.S. Lee, C.B. Park, Adv. Funct. Mater. 20 (2010) 2132.
[42] J.H. Kim, M.S. Park, J.H. Song, D.J. Byun, Y.J. Kim, J.S. Kim, J. Alloys Compd. 517 (2012) 20.
[43] A.R. Armstrong, M. Holzapfel, P. Novak, C.S. Johnson, S.H. kang, M.M. Thackeray, P.G. Bruce, J. Am. Chem. Soc. 128 (2006) 8694.